Article

Application of Molecular Absorption Properties of Horseradish Peroxidase for Self-Indicating Enzymatic Interactions and Analytical Methods

Vanesa Sanz, Susana de Marcos, Juan R. Castillo, and Javier Galbn

J. Am. Chem. Soc., **2005**, 127 (3), 1038-1048• DOI: 10.1021/ja046830k • Publication Date (Web): 31 December 2004

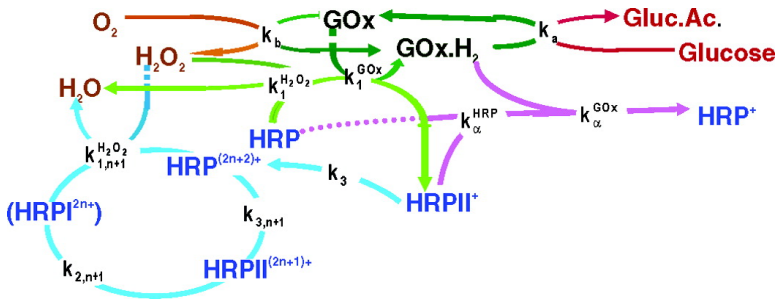

More About This Article

Additional resources and features associated with this article are available within the HTML version:

- Supporting Information
- Links to the 1 articles that cite this article, as of the time of this article download
- Access to high resolution figures
- Links to articles and content related to this article
- Copyright permission to reproduce figures and/or text from this article

View the Full Text HTML

J|A|C|S
ARTICLES
Published on Web 12/31/2004

Application of Molecular Absorption Properties of Horseradish Peroxidase for Self-Indicating Enzymatic Interactions and Analytical Methods

Vanesa Sanz,[†] Susana de Marcos,[†,‡] Juan R. Castillo,[†] and Javier Galbán*[,†,‡]

Contribution from the GEAS, Analytical Chemistry Department, Faculty of Sciences, University of Zaragoza, Zaragoza-50009, Spain, and Institute of Nanotechnology, University of Zaragoza, Zaragoza-50009, Spain

Received May 28, 2004; E-mail: jgalban@unizar.es.

Abstract: In this paper an in depth study is presented of the use of the horseradish peroxidase (HRP) enzyme as a self-indicating biorecognition reagent in UV−vis molecular absorption spectrometry. The HRP/H_2O_2 reaction mechanism in the absence of an external substrate has been clarified, and the interaction between HRP and glucose oxidase (GOx) has been studied. It has been demonstrated that GOx can act as a substrate of HRP; in both cases the kinetic constants have been obtained and mathematical models have been developed. Second, the HRP/H_2O_2 reaction is used to follow a H_2O_2-producing enzymatic reaction, the glucose reaction with GOx being used as a model. As an application of this, two methodologies have been proposed for glucose determination: with or without previous incubation of glucose with GOx. In both cases mathematical models relating HRP absorbance changes to glucose concentration have been developed and tested; both methods have been optimized, analytically characterized, and tested for glucose determination in samples. The methodology described could be applied to other heme-proteins and to other H_2O_2-producing enzymatic reactions. The models permit the reaction constants to be calculated. From the analytical chemistry point of view the models allow the prediction of the method sensitivity for other analytes involved in this type of reaction if the kinetic constants are known and can be used in the design of optical sensors.

1. Introduction

The design and optimization of analytical methods for organic compounds of interest in environmental or biological samples is one of the most important problems of analytical chemistry today. As the majority of these compounds do not display sufficient spectroscopic or electroanalytical properties for their direct determination, it is necessary to use indirect methods based on the use of a reagent. An ideal reagent would provide chemical and spatial selectivity for the analyte to be determined and would also be able to yield an analytical signal during the reaction. The use of proteins as biorecognition reagents is a good choice because of their reasonably good selectivity (both chemical and spatial), but their spectroscopic properties either are not well-known or have not been able to be used until recently.

Several methodologies have emerged in recent years based on the spectroscopic properties of proteins, mainly fluorescence (intrinsic or extrinsic, obtained after a chemical modification with a fluorophore). In our opinion, the most significant are based on the following:

(a) The use of regulator or transport proteins. After joining to the corresponding molecule (normally in the folding area of the protein) these proteins suffer a conformational change which can be detected if a fluorophore is previously linked in the folding area (chemically[1]or by direct mutagenesis[2,3]). In addition, good results have been obtained after fusing the "reagent protein" with the green fluorescence protein,[4] whose fluorescence also changes after linking. In this context, works by Cass,[1,2] Hellinga,[3] or Daunert[4] can be highlighted

(b) The use of apoenzymes. This methodology has been developed by Lakowicz and D'Auria.[5,6] According to these authors, after the substrate−enzyme linkage, changes are observed in the intrinsic fluorescence of some enzymes or of some modified enzymes with fluorophores (chemically or by direct mutagenesis).

(c) The use of flavoenzymes whose fluorescence changes during the enzymatic reaction. This methodology was first proposed by Wolfbeis and Trettnak,[7] using the FAD fluorescence changes during the reaction. In recent years our group has been developing a line of research based on both the intrinsic (due to tryptophan)[8,9] and the extrinsic (a chemically linked

[†] Analytical Chemistry Department, University of Zaragoza.
[‡] Institute of Nanotechnology, University of Zaragoza.

(1) Zhou, L. Q.; Cass, A. E. G. *Biosens. Bioelectron.* **1991**, *6*, 445−450.
(2) Gilardi, G.; Mei, G.; Rosato, N.; Finazzi, A.; Cass, A. E. G. *Protein Eng.* **1997**, *10*, 479−486.
(3) Marvin, J. S.; Hellinga, H. W. *J. Am. Chem. Soc.* **1998**, *120*, 7−11.
(4) Dikici, E.; Sapna, K.; Daunert, S. *Anal. Chim. Acta* **2003**, *500*, 237−245.
(5) D'Auria, S.; Lakowicz, J. R. *Curr. Opin. Biotechnol.* **2001**, *12*, 99−104.
(6) D'Auria, S.; di Cesare, N.; Gryczynski, Z.; Gryczynski, I.; Rossi, M.; Lakowicz, J. R. *Anal. Biochem.* **2002**, *303*, 138−144.
(7) Trettnak, W.; Wlfbeis, O. S. *Fresenius'J. Anal. Chem.* **1989**, *334*, 427−430.

10.1021/ja046830k CCC: $30.25

fluorophore)[10,11] fluorescence changes during the enzymatic reaction of this type of enzyme. Our conclusion is that both the intrinsic and the chemically modified fluorescence of the enzymes change due to an energy transfer process involving the FAD as an acceptor or a donor, respectively. For this reason, the methodology is only applicable to analytes which can be involved in reaction with flavoenzymes.

The molecular absorption properties of enzymes has scarcely been used as an analytical signal. However, many metal−enzymes (mainly those containing iron[12] or copper[13]) have spectrophotometric properties that deserve to be studied and evaluated as candidates for analytical signals. As is known, peroxidase (HRP) catalyses the oxidation of many substrates (S) (phenols, aromatic amines and aromatic sulfonates) with H_2O_2 according to the following general scheme:

$$H_2O_2 + S_{reduced} \leftarrow HRP \rightarrow 2H_2O + S_{oxidized}$$

From the mechanistic point of view the process is complicated,[14−16] but it can be summarized as follows. HRP can be considered to consist of the heme catalytic center and the surrounding proteic. In the native state of peroxidase, the heme group contains Fe(III). The different intermediates formed during the HRP reaction with H_2O_2 are shown in the following scheme:

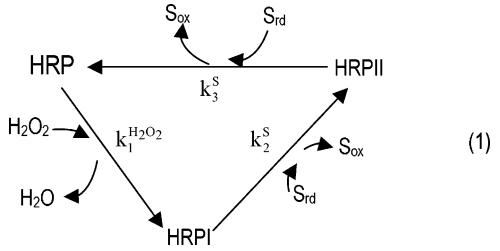

During the oxidation step HRP reacts with H_2O_2 yielding an intermediate usually known as compound I and denoted as HRPI, in which the formal oxidation state of the heme group is 5+ (throughout we will refer to any HRP in which the oxidation state of the heme group is 5+ as HRPI). The reduction step is carried out by the S in two stages:[17] first, HRPI is semireduced to the so-called compound II (HRPII), the formal oxidation state of the heme group being 4+ (throughout we will refer to any HRP in which the oxidation state of the heme group is 4+ as HRPII), and second HRPII is reduced to HRP. The reported value for k_1 ranges from 1.0×10^7 to 1.5×10^7 M^{-1} s^{-1}.[17−22] As regards k^S_2 and k^S_3, values have been reported for some substrates; from these values the last step is the limiting step of the overall process.[17,18,22]

Contrary to what might be expected we have observed the reaction of H_2O_2 with HRP in the absence of conventional substrates. Accordingly, first, this paper develops a mathematical and kinetic model for this reaction; second, the interaction between HRP and a flavoenzyme, glucose oxidase (GOx), is studied; third, methods for the glucose enzymatic determination are presented, based on the reaction between the HRP and the H_2O_2 previously generated in the enzymatic oxidation of glucose with GOx. The glucose determination is here used as a reaction model, but this methodology can be applied to any other H_2O_2 producing enzymatic reaction. An extensive theoretical study is presented which relates the absorbance changes with the analyte and the enzyme concentrations; in the light of this study, it has been possible to clarify the mechanism of the HRP reaction and obtain some experimental rate constants. As regards the specific application of this method for glucose, several advantages arise compared to those based on protein or enzyme fluorescence: (a) there is a greater sensitivity, (b) it is less prone to spectral interferences (depending on the wavelength used), and (c) it is nondependent on the O_2 concentration.

2. Experimental Section

2.1. Instruments. The molecular absorption measurements were carried out in a Hewlett-Packard 8452A diode-array spectrometer and in a Perkin-Elmer Lambda 5 spectrometer (using a spectral bandwidth of 2 nm). Quartz cells of 1 cm optical pathway were used.

The fluorescence measurements were carried out in a PTI (Photon Instrument Technology) QuantaMaster model QM2004 modular luminometer, using quartz cells of 1 cm optical pathway.

2.2. Materials. Buffer solutions of different pHs were prepared from solid KH_2PO_4 and solid Na_2HPO_4.

Horseradish peroxidase (HRP), EC 1.11.1.7 (Sigma P-8125), was of 148 IU mg^{-1} of lyophilised solid. Glucose oxidase (GOx) was taken from *Aspergillus niger*, EC 1.1.3.4 (Sigma G-7141), and was of 246 IU mg^{-1} of lyophilised solid. Enzyme solutions were prepared by dissolving the solid in the above-mentioned buffer solutions.

Glucose (G) stock solutions were prepared by dissolving the appropriate amount of β-D-(+)-glucose (Sigma G-5250) in the phosphate buffer solution.

Synthetic serum is obtained by reconstitution of ACCUTROL Normal (Accumark Controls, SIGMA A2034) with 5 mL bidistilled water.

2.3. Procedure for Glucose Determination. (i) Without Previous Incubation. Glucose solution (1400 μL) in phosphate buffer (pH 6) and HRP solution (500 μL, 800 IU mL^{-1}, 1.2×10^{-4}M) were placed in the measurement cuvette, and the absorbance value (Abs_0) was obtained. After 20 s, 100 μL of glucose oxidase solution (500 IU mL^{-1}, 1.0×10^{-5}M) were added to the cuvette. At 420 or 560 nm, a sharp increase in the absorbance to a maximum value (Abs_{max}) was observed, followed by a gradual decrease in absorbance. The $Abs_{max} - Abs_0$ difference was used as the analytical parameter. For glucose determination in the synthetic serum, 5 μL of the reconstituted sample added to 1400 μL of buffer solution or glucose standard solution for the recovery study were placed in the cuvette, and the method followed as described above.

(8) Galbán, J.; de Marcos, S.; Castillo, J. R. *Anal. Chem.* **1993**, *65*, 3076−3080.
(9) Sierra, J. F.; Galbán, J.; Castillo, J. R. *Anal. Chem.* **1997**, *69*, 1471−1476.
(10) Galbán, J.; Andréu, Y.; Sierra, J. F.; de Marcos, S.; Castillo, J. R. *Luminescence* **2001**, *16*, 199−210.
(11) Sierra, J. F.; Galbán, J.; de Marcos, S.; Castillo, J. R. *Anal. Chim. Acta* **2000**, *414*, 33−41.
(12) Blumberg, W. E.; Peiscich, J.; Wittenberg, B. A.; Wittenberg, J. A. *J. Biol. Chem.* **1968**, *243*, 1854−1862.
(13) Zoppellaro, G.; Sakurai, T.; Huang, H. *J. Biochem.* **2001**, *129*, 949−953.
(14) Murielle, D.; Limoges, B.; Moiroux, J.; Savéant, J. M. *J. Am. Chem. Soc.* **2002**, *124*, 240−253.
(15) Dunford, H. B. *Comprehensive Biological Catalysis*; Sinnot, M., Ed.; Academic Press: London, 1998; pp 196−237.
(16) Filizola, M.; Loew, G. H. *J. Am. Chem. Soc.* **2000**, *122*, 18−25.
(17) Ignatenko, O. V.; Gazaryan, I. G.; Mareeva, E. A.; Chubar, T. A.; Fechina, V. A.; Savitsky, P. A.; Rojkova, A. M.; Tishkov. V. I. *Biochemistry* **2000**, *65*, 583−587.
(18) Gazaryan, I. G.; Chubar, T. A.; Ignatenko, O. V.; Mareeva, E. A.; Orlova, M. A.; Kapeliuch, Y. L.; Savitsky, P. A.; Rojkova, A. M.; Tishkov. V. I. *Biochem. Biophy. Res. Commun.* **1999**, *262*, 297−301.
(19) English, A. M.; Tsaprailis, G. In *Advances in inorganic chemistry;* Sykes, A. G, Ed.; Academic Press: 1995; Vol. 43, pp 79−125.
(20) Morimoto, A.; Tanaka, M.; Takahashi, S.; Ishimori, K.; Hori, H.; Morishima, I. *J. Biol. Chem.* **1998**, *273*, 14763−14760.
(21) Furtmüller, P. G.; Arnhold, J.; Jantschjo, W.; Pichler, H.; Obinger, C. *Biochem. Biophys. Res. Commun.* **2003**, *301*, 551−557.
(22) Nagano, S.; Tanaka, M.; Ishimori, K.; Watanabe, Y.; Morishima, I. *Biochemistry* **1996**, *35*, 14251−14258.

Scheme 1. HRP Cycle

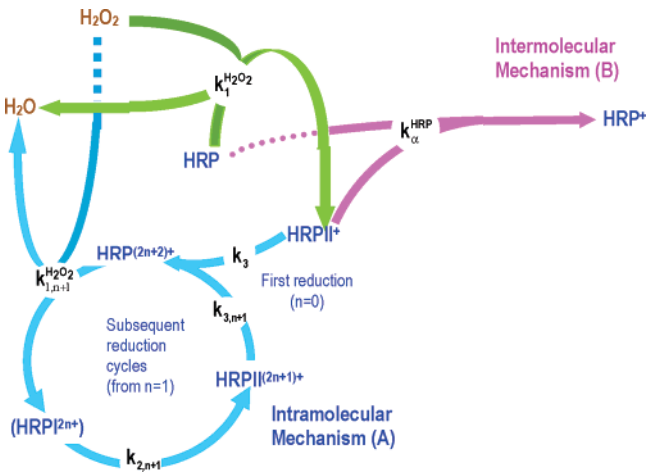

(ii) With Previous Incubation. Glucose solution (1400 μL) in phosphate buffer (pH 6) and glucose oxidase solution (100 μL, 700 IU mL^{-1}) were placed in the cuvette. After 5 min (incubation time), 500 μL of HRP solution (800 IU mL^{-1}) were added to the measurement cuvette, and the absorbance value (Abs_{max}) was obtained. At 420 or 560 nm, a decrease in the absorbance to a value Abs_0 is observed. For glucose determination in commercial fruit juices, samples are conveniently diluted in bidistilled water (or glucose standard solution for the recovery study) and submitted to the same procedure.

3. Results and Discussion

3.1. Reaction between HRP and Hydrogen Peroxide. (i) Kinetic Pathways in HRP/H_2O_2 Reaction and Molecular Absorption Measurements. According to the bibliography and our own observations, the reduction step in reaction 1 can take place, in the absence of a conventional substrate, by means of the surrounding proteic part of the peroxidase (which will be called P throughout), by both an intramolecular (the P part belonging to the same HRP molecule) and an intermolecular (the P part belonging to another HRP molecule present in the medium) reduction mechanism. During intramolecular reduction (Scheme 1, zone A), electrons are transferred, after HRPI formation, from the aromatic amino acids of the same enzyme to the heme group.[23] This process follows a two-step mechanism:[19,20]

$$\mathrm{HRPI} = (k_2) \Rightarrow \mathrm{HRPII}^{+}$$

$$\mathrm{HRPII}^{+} = (k_3) \Rightarrow \mathrm{HRP}^{2+}$$

(throughout we will represent the positive charge of the P part as a superscript in the corresponding peroxidase form). Although numerical values for k_2 and k_3 have not been reported, it is known that the first step is very fast,[17] so it is possible to group this reaction with that in which HRP reacts with hydrogen peroxide to form HRPI. The HRP^{2+} can then react again with other H_2O_2 molecules until the P part of the same HRP is unable to transfer more electrons to the heme group. It has been suggested in the bibliography[18] that the main difference betweenthe cycles is the constant rate values; in each new oxidation/reduction cycle the constant rates are slower than in the previous cycle so the intermediate $HRPI^{((2n+2)+)}$ species can be detected (numerical values for these constants have also not been reported).

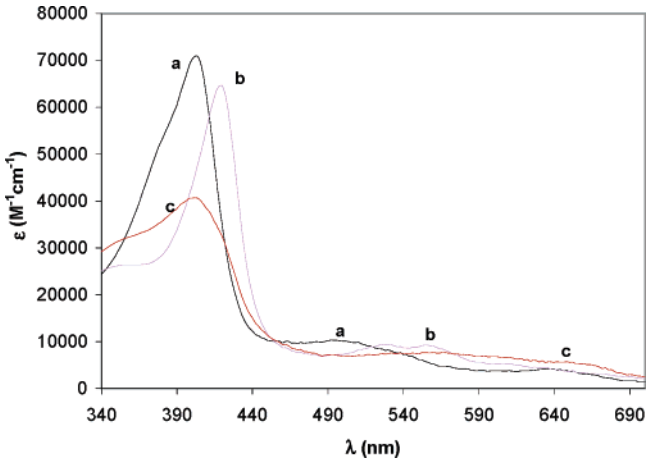

Figure 1. Absorption spectrum of horseradish peroxidase: (a) HRP, (b) HRPII, (c) HRPI.

In the intermolecular mechanism (Scheme 1, zone B), the electron is transferred from the aromatic amino acids located in another HRP molecule. The lower the oxidation state of the P part, the lower the reaction probability (constant rate), so the main reaction of this mechanism is likely to be:

$$\mathrm{HRPII}^{+} + \mathrm{HRP} = (k_{\alpha}^{\mathrm{HRP}}) \Rightarrow 2\mathrm{HRP}^{+}$$

The $k_{\alpha}^{\mathrm{HRP}}$ value has not been reported.

HRP has a complex molecular absorption spectrum; only the visible region (from 340 to 700 nm) will be considered here. In this zone the spectrum depends on the heme group oxidation state[12,24] (see Figure 1) in such a way that changes in this region can be used to follow the enzymatic reaction. All the HRP forms have the same spectra (maxima at 402 nm, 500 nm, with a shoulder at 540 nm, and 638 nm), so that $\epsilon_{\mathrm{HRP},\lambda} \approx \epsilon_{\mathrm{HRP}^{+},\lambda} \approx \epsilon_{\mathrm{HRP}^{2+},\lambda} \approx$ .....

The same is valid for HRPI species (maxima at 402 nm, 550, 618, and 648 nm) and HRPII species (maxima at 420, 527, and 554 nm). In these spectra, the isosbestic points between two or three species are as important as the maxima. There are isosbestic points between HRP/HRPI species at 355, 420, and 532 nm, between HRP/HRPII species at 409 and 514 nm, between HRPII/HRPI species at 395 and 582 nm, and between the three kinds of species at 450 nm. The isosbestic points could be important because from the kinetic point of view they enable us to follow the variation of the concentration of a particular redox state of peroxidase and from the analytical point of view they can be used as reference wavelengths when needed. All the assays have been performed by measuring all the spectra; for the sake of simplicity, results at one wavelength (420 nm) will be presented in most cases.

(ii) Study of the HRP/H_2O_2 Reaction I: Excess of HRP. In light of the aim of the work, this case is of great interest because it is easier to relate the absorbance variations with H_2O_2

(23) We have been able to observe this electron transference by monitoring the HRP tryptophan fluorescence (λ_{exc} = 280 nm and λ_{fl} = 340 nm); during the reaction, a sharp decrease in intensity was observed due to the tryptophan oxidation.

(24) Pina, D. G.; Shnyrova, A. V.; Gavilanes, F.; Rodríguez, A.; Leal, F.; Roig, M. G.; Sakharov, I. Y.; Zhadan, G. G.; Villar, E.; Shnyrov, V. L. *Eur. J. Biochem.* **2001**, *268*, 120−126.

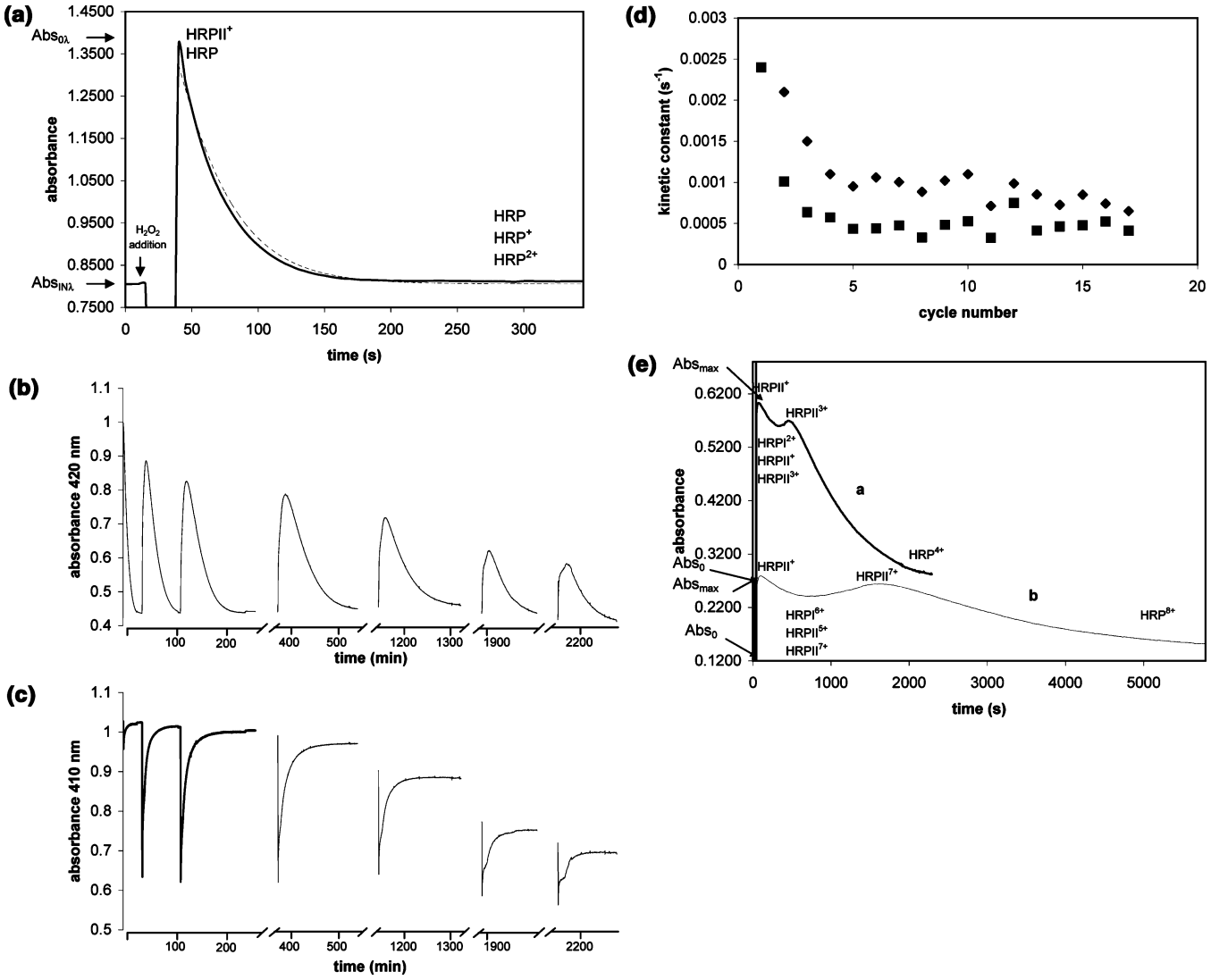

Figure 2. (a) Abs variation at 420 nm during reaction when HRP exceeds H_2O_2 (pH = 6, [HRP] = 4.5×10^{-5} M, and $[H_2O_2]_0 = 1.5 \times 10^{-5}$ M). The broken line shows the theoretical curve obtained after the application of mathematical model 7. Absorbance variation at (b) the HRP/HRPI isosbestic point (420 nm) and (c) the HRP/HRPII isosbestic point (410 nm), when HRP is made to react with several stoichiometric aliquots of H_2O_2. Only the 1st, 2nd, 3rd, 5th, 10th, 15th, and 17th cycles are shown. The initial absorbance at 420 nm for each cycle does not change, but at 410 nm it decreases. This is because an accumulation of HRPI is produced after each cycle, this being an inactive form of HRP for the subsequent cycle (pH = 6, $[HRP]_0 = [H_2O_2]_0 = 3.0 \times 10^{-5}$ M). (d) Kinetic constants $k_{2,n+1}$ (◆) and $k_{3,n+1}$ (■) obtained from the results given in Figure 2B. (e) Absorbance variation at 420 nm (pH = 6) during peroxidase reaction when H_2O_2 exceeds HRP. (a) $[HRP]_0 = 1.6 \times 10^{-5}$ M and $[H_2O_2]_0 = 3 \times 10^{-5}$ M. (b) $[HRP]_0 = 8.3 \times 10^{-6}$ M and $[H_2O_2]_0 = 3 \times 10^{-5}$ M.

concentrations, and the absorbance changes are more sensitive to changes in H_2O_2 (or related species) concentrations.

When HRP is in excess relating to H_2O_2, at the beginning of the reaction all of the H_2O_2 will react with the HRP which is converted to $HRPII^+$, so an excess of HRP remains in solution with $HRPII^+$. Afterward, this compound can be reduced by both the intramolecular reaction yielding HRP^{2+} (only the first reduction will be produced) and the intermolecular process yielding HRP^+, so the concentrations of HRP and $HRPII^+$ decrease and the concentrations of HRP^+ and HRP^{2+} increase. This produces a global decrease in the absorbance at 420 nm. The $\Delta Abs_{t,\lambda}$ (see below) gives the concentration of $HRPII^+$ which remains in solution. Figure 2A shows the absorbance versus time variation at 420 nm obtained for this case.

According to the mechanism (Scheme 1 and Figure 2A) at the beginning of the reaction (and during a large part of the enzymatic reaction when working with a high excess of HRP) the mass balance can be simplified to

$$[HRP]_0 = [HRP]_t + [HRP^+]_t + [HRP^{2+}]_t + [HRPII^+]_t \approx [HRP]_t + [HRPII^+]_t \quad (2)$$

$[HRP]_0$ being the initially added HRP concentration.

Given the reaction mechanism described, H_2O_2 quickly reacts with HRP yielding $HRPII^+$, so

$$[HRPII^+]_{t=0} = [H_2O_2]_0 \quad (3)$$

The $HRPII^+$ consumption rate is then given by

$$\frac{d[HRPII^+]}{dt} = -k_3[HRPII^+]_t - k_\alpha^{HRP}[HRPII^+]_t[HRP]_t \quad (4)$$

After eqs 2−4 were combined and the differential equation was resolved, the following expression can be obtained,

$$[\mathrm{HRPII}^+]_t = \frac{A[\mathrm{H_2O_2}]_0 10^{-At}}{A - k_\alpha^{\mathrm{HRP}}[\mathrm{H_2O_2}]_0(1 + 10^{-At})} \quad (5)$$

A being

$$A = k_3 + k_\alpha^{\mathrm{HRP}}[\mathrm{HRP}]_0$$

which represents the overall maximum rate for HRP reduction.

The absorbance variation observed at any λ at any moment during the reaction will be given by

$$\Delta\mathrm{Abs}_{t,\lambda} = \mathrm{Abs}_{t,\lambda} - \mathrm{Abs}_{\mathrm{IN},\lambda}$$

$\mathrm{Abs}_{\mathrm{IN},\lambda}$ being the HRP absorbance before the reaction. Considering eq 2, we obtained the following equation:

$$\Delta\mathrm{Abs}_{t,\lambda} = \Delta\epsilon_\lambda[\mathrm{HRPII}^+]_t \qquad (\Delta\epsilon_\lambda = \epsilon_{\mathrm{HRPII}^+} - \epsilon_{\mathrm{HRP}}) \quad (6)$$

After substituting eq 5 in eq 6 and reorganizing, we obtained

$$\frac{1}{\Delta\mathrm{Abs}_{t,\lambda}} = \frac{k_\alpha^{\mathrm{HRP}}}{\Delta\epsilon_\lambda A}(1 - 10^{At}) + \frac{10^{At}}{\Delta\epsilon_\lambda}\frac{1}{[\mathrm{H_2O_2}]_0} \quad (7)$$

This equation relates the inverse of the absorbance changes at any wavelength and at any moment during the reaction (condition 2 always being fulfilled) with the initial hydrogen peroxide concentration. A much simplified equation for eq 7 can be obtained when $t = 0$

$$\Delta\mathrm{Abs}_{0,\lambda} = \Delta\epsilon_\lambda[\mathrm{H_2O_2}]_0 \quad (8)$$

Examples of the fulfilment of eq 8 are given in Table 1; the slopes of the calibration lines match very well with the molecular absorptivity values (Figure 1) as the equation predicts.

To calculate k_3 and k_α^{HRP}, the Abs versus time profiles (similar to those shown in Figure 2A) obtained for three different H_2O_2 concentrations and three different HRP concentrations were fitted to eq 7. The following values were obtained:

$$k_3 = 0.0030 \pm 0.0011\ \mathrm{s^{-1}} \qquad k_\alpha^{\mathrm{HRP}} = 224 \pm 37\ \mathrm{M^{-1}\ s^{-1}} \quad (9)$$

As has been indicated, an exact value for k_3 and k_α^{HRP} has not been reported, only an approximate value for the overall reduction of HRP in the absence of reductive substrates of about 10^{-2} $\mathrm{s^{-1}}$.[20] As can be seen, the $k_3 + k_\alpha^{\mathrm{HRP}}$ ($[\mathrm{HRP}]_o - [\mathrm{H_2O_2}]_o$) obtained, which is an approximation of the overall kinetic constant for HRP reduction in accordance with the proposed mechanism, is in the range of the reported estimation. From the values obtained for k_3 and k_α^{HRP} and eq 7, it is possible to obtain the theoretical variation of absorbance as a function of time (see Figure 2A, broken line). As can be seen, the theoretical curve matches the experimental curve very well, which confirms the aproximation 2.

The model described in eq 7 can be applied for kinetic constant determination for other heme proteins. Analytically, eq 8 provides the basis of a simple analytical method for H_2O_2 determination based on the absorbance changes of HRP.

(iii) Study of the HRP/H_2O_2 Reaction I: Excess of H_2O_2. In this case the intramolecular reduction predominates, and each HRP molecule reacts with several H_2O_2 molecules. Figure 2B shows the absorbance variation versus time at 420 nm (an isosbestic point for HRP/HRPI) and 410 nm (an isosbestic point for HRP/HRPII), when HRP is made to react with several stoichiometric aliquots (relating to the Heme group of HRP) of H_2O_2. These results agree with Scheme 1. After the first H_2O_2 addition (first cycle), the compound HRP is converted directly into HRPII^+, so the absorbance at 410 nm does not change. For subsequent cycles, the HRP^{2n+} is first converted into HRPI^{2n+} (deduced from the decrease in the absorbance at 410 nm), then into $\mathrm{HRPII}^{(2n+1)+}$ (both wavelengths increase: the absorbance at 410 nm returns to the initial value and the absorbance at 420 nm reaches the maximum), and finally into $\mathrm{HRP}^{(2n+2)+}$ (the trend of the absorbance curve as a function of time at 410 nm does not change, while that at 420 nm decreases). According to our experiment, each HRP molecule is able to produce at least 17 cycles; from that point on, the absorbance changes are very low and it is difficult to follow the process accurately. A mathematical process gives equations for obtaining the $k_{2,n+1}$ and $k_{3,n+1}$ constants from the absorbance versus time variations.

Table 1. Calibration Curves for H_2O_2 Obtained Working with Absorbances Measured at Different Wavelengths ($[\mathrm{HRP}] = 2.1 \times 10^{-5}$ M and pH = 6); in All Cases the Linear Range Is Obeyed from 2.5×10^{-6} M to 2.5×10^{-5} M

wavelength, nm	slope, $\mathrm{M^{-1}\ cm^{-1}}$	intercept	r
420	34 570	−0.0193	0.996
490	3579	0.0061	0.996
560	3744	−0.0023	0.996

The absorbance increase at 410 nm in each cycle follows the equation:

$$\ln\frac{\mathrm{Abs}_0 - \mathrm{Abs}_t}{\mathrm{Abs}_0} = \ln\frac{\Delta\epsilon_{\mathrm{HRP/HRPI}}}{\epsilon_{\mathrm{HRP}}} - k_2 t$$

$\Delta\epsilon_{\mathrm{HRP/HRPI}}$ being the molar absorptivity difference between both species and t being the time of each cycle. The absorbance decrease at 420 nm in each cycle follows the equation:

$$\ln\frac{\mathrm{Abs}_t - \mathrm{Abs}_0}{\mathrm{Abs}_0} = \ln\frac{\Delta\epsilon_{\mathrm{HRP/HRPII}}}{\epsilon_{\mathrm{HRP}}} - k_3(t - t_{\max})$$

$\Delta\epsilon_{\mathrm{HRP/HRPII}}$ being the molar absorptivity difference between both species and t being the time of each cycle, taking $t_{\max}$ as the time of the maximum in each cycle. From these equation the k_2 and k_3 for each cycle can be estimated (Figure 2C). Both constants diminish as the number of cycles increases, as predicted by the kinetic model.

From the analytical chemistry point of view, the question is how the absorbance at a given wavelength (for example, 420 nm) changes when HRP is added to a solution containing an excess of H_2O_2. This is represented in Figure 2D; the result obtained can be explained as before. A mathematical model has also been developed for this case. However, as a different equation is necessary to describe each stretch of the curve (Figure 2D), the model is very complex and is not fully presented.

However, two conclusions can be highlighted:

(1) The first maximum in Figure 2D depends only on $[\mathrm{HRP}]_0$ according to the equation

$$\Delta Abs_{0,\lambda} = \Delta\epsilon_{\lambda}[HRP]_0$$

(2) The absorbance at the first maximum and the minimum at 420 nm are related by

$$\frac{Abs_{max,420} - Abs_{min,420}}{Abs_{min,420}} = \frac{k_{3,n}(\epsilon_{HRPII} - \epsilon_{HRPI})}{k_{2,n+1}\epsilon_{HRPII}}(n+1) - \frac{k_{3,n}(\epsilon_{HRPII} - \epsilon_{HRPI})}{k_{2,n+1}\epsilon_{HRPII}}\frac{[H_2O_2]_0}{[HRP]_0}$$

n being the number of the last complete cycle (n+1, refers to the cycle number in which the stoichiometric excess of H_2O_2 relating to HRP is consumed or the last cycle number for a stoichiometric mix). The experimental ($Abs_{max,420} - Abs_{min,420}$/$Abs_{min,420}$) values obtained for the two $[H_2O_2]_0/[HRP]_0$ shown in Figure 2 are 0.071 (line a) and 0.133 (line b) which fit very well with the theoretical values 0.093 (line a) and 0.131 (line b) derived from the application of the previous equation.

From the analytical point of view, the changes in absorbance are also related to $[H_2O_2]_0$ but in a more complicated way. However from the kinetic point of view the expression can be more interesting.

3.2. Interaction of HRP with the Flavoenzyme Glucose Oxidase. (i) General Mechanism. Glucose oxidase catalyses glucose oxidation with O_2 by a well-known mechanism than can be expressed in a simplified way as[9]

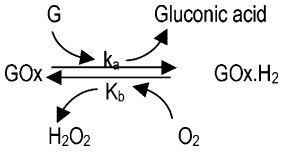

GOx is the enzyme with the cofactor in the oxidized form (FAD), GOx.H_2 is the enzyme with the cofactor in the reduced form (FAD.H_2), and G is the glucose. When this reaction is carried out in the presence of HRP, it is possible to determine glucose by monitoring the changes in the absorbance of the HRP in such a way that it can act simultaneously as both an enzyme and a colorimetric reagent. This will be discussed further in sections 3.3 and 3.4, but here it is necessary to say something about GOx and HRP interaction.

In their natural state both enzymes present redox properties suggesting a possible reaction between them: HRP can be oxidized, and GOx reduced in such a way that GOx could act as a "substrate" for HRP. However, if this reaction occurs, the whole process will be very complicated because after reduction GOx can be regenerated by the dissolved O_2 (the saturation concentration in water at 25 °C is 2×10^{-4} M) in the same way as yielding a H_2O_2 molecule which can react with HRP. Moreover, as GOx presents aromatic amino acid residues (in much greater quantities than HRP), it can contribute to the intermolecular regeneration of HRP (see Scheme 2).

Figure 3A shows a sequence of molecular absorption spectra obtained after mixing HRP and GOx in similar concentrations. If the GOx molecular absorption is subtracted from this figure, the spectrum sequence obtained corresponds in shape (not in velocity) to the HRP transformation by H_2O_2 previously described. This result demonstrates that GOx acts as a substrate

Scheme 2. GOx/HRO Combined Cycle

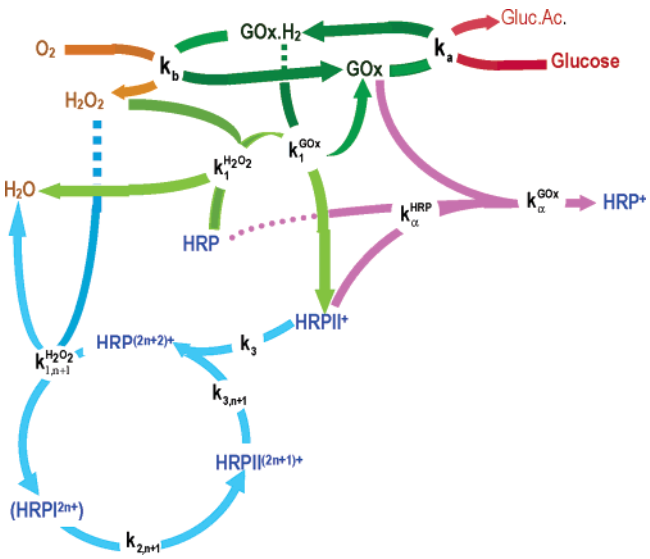

of HRP and that GOx is the predominant form of glucose oxidase in the solution. However, a comparison of Figures 3A (upset) and 2A suggests that the kinetic constants for the GOx/HRP reaction are lower than those for the H_2O_2/HRP reaction (the increase in absorbance at 420 nm in Figure 3A is slower than in Figure 2A). The k_1^{GOx} and k_α^{GOx} values must now be calculated.

(ii) Kinetic Constants Measurement I → k_1^{GOx}. According to Scheme 2, and in the absence of glucose, the $[HRPII]^+$ variation rate is given by

$$\frac{d[HRPII^+]}{dt} = \underbrace{k_1^{GOx}[GOx]_t[HRP]_t + k_1^{HRP}[H_2O_2]_t[HRP]_t}_{\text{formation by reaction with GOx and } H_2O_2} - \underbrace{k_3[HRPII^+]_t}_{\text{intramolecular mechanism}} - \underbrace{k_\alpha^{HRP}[HRPII^+]_t[HRP]_t - k_\alpha^{GOx}[HRPII^+]_t[GOx]_t}_{\text{intermolecular mechanism with HRP and GOx}} \quad (10)$$

To solve the differential equation, in addition to the mass balance for peroxidase, two general considerations can be made: (1) The stationary state condition for H_2O_2 can be applied (H_2O_2 is consumed as it is produced), and when $[O_2]_0 > [GOx]_0$, the stationary state can also be applied for $[GOx.H_2]$;[9] (2) as GOx.H_2 is quickly reoxidized, GOx is the predominant species of glucose oxidase in the solution. These considerations transform eq 10 into

$$\frac{d[HRPII^+]}{dt} = 2k_1^{GOx}[GOx]_0[HRP]_0 - [HRPII^+]_t(2k_1^{GOx}[GOx]_0 + k_3 + k_\alpha^{HRP}[HRP]_0 + k_\alpha^{GOx}[GOx]_0) + k_\alpha^{HRP}[HRPII^+]_t^2 \quad (11)$$

At the beginning of the reaction (approximately the first 200 s), the concentration of the $HRPII^+$ produced is significantly lower than the HRP, so that $][HRPII^+]_t^2$ can be discarded. With this consideration, resolving the differential eq 11 and trans-

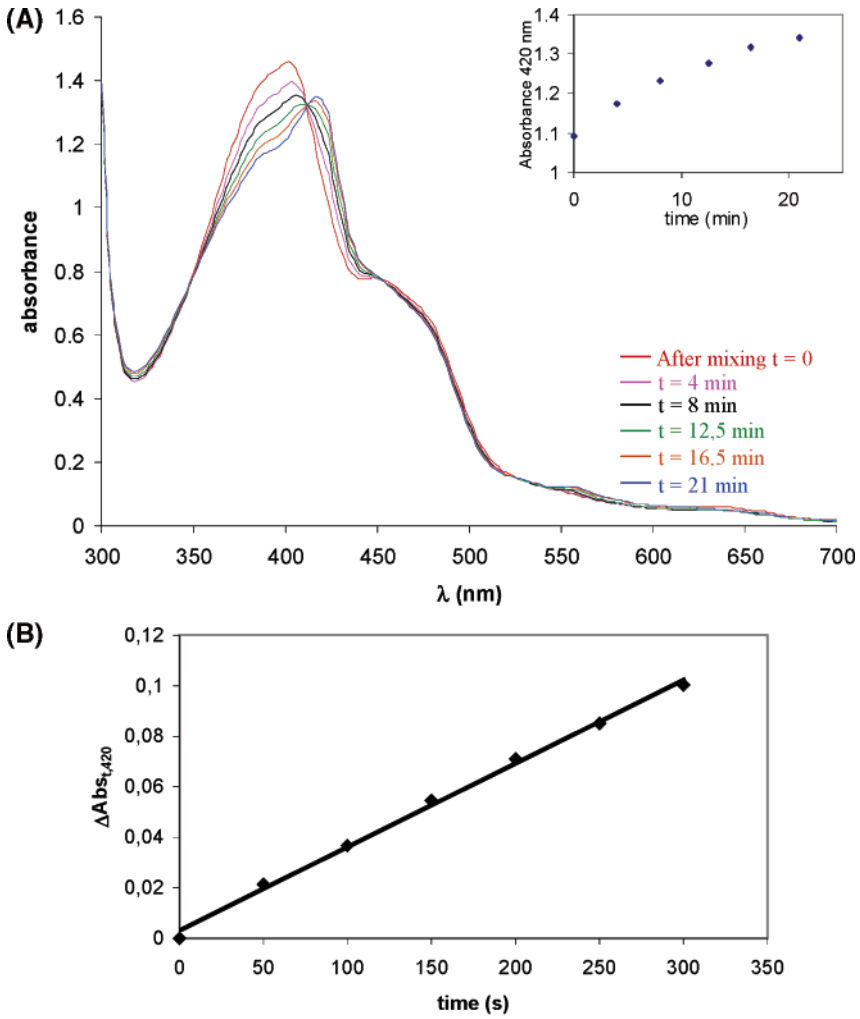

Figure 3. (A) Variation of the absorption spectrum of a mixture containing HRP (3.01×10^{-5} M) and glucose oxidase (3.09×10^{-5} M) in similar concentrations (pH = 6). Inset: absorbance variation as a function of time at a fixed wavelength (420 nm). (B) Fit of experimental results to the model proposed for the calculus of the kinetic constant k_1^{GOx}. The experimental data fit the following equation $\Delta Abs_{t,420} = (3.31 \times 10^{-4})t + 3.10 \times 10^{-3}$ (r = 0.998).

forming $[HRPII^+]_t$ into absorbance at 420 nm (see eq 6) give the following equation:

$$\Delta Abs_{t,420} = \Delta\epsilon_{420} \frac{2k_1^{GOx}[GOx]_0[HRP]_0}{k_3 + k_\alpha^{HRP}[HRP]_0 + k_\alpha^{GOx}[GOx]_0 + 2k_1^{GOx}[GOx]_0} \times (1 - \exp[-(k_3 + k_\alpha^{HRP}[HRP]_0 + k_\alpha^{GOx}[GOx]_0 + 2k_1^{GOx}[GOx]_0)t])$$

The sequence of the spectrum shown in Figure 3A suggests that the exponent is small so the following approximation can be made:

$$1 - \exp[-(k_3 + k_\alpha^{HRP}[HRP]_0 + k_\alpha^{GOx}[GOx]_0 + 2k_1^{GOx}[GOx]_0)t] = (k_3 + k_\alpha^{HRP}[HRP]_0 + k_\alpha^{GOx}[GOx]_0 + 2k_1^{GOx}[GOx]_0)t \quad (12)$$

and the previous equation is transformed in

$$\Delta Abs_{t,420} = \Delta\epsilon_{420} 2k_1^{GOx}[GOx]_0[HRP]_0 t \quad (13)$$

The fit of the experimental results to eq 13 is presented in Figure 3B. The following value was obtained from five replicates of the test:

$$k_1^{GOx} = 5.9 \pm 0.5\ M^{-1}\ s^{-1}$$

(iii) Kinetic Constants Measurement II → k_α^{GOx}. To obtain the k_α^{GOx} value, it is important to avoid both the reaction in which H_2O_2 is formed and the intermolecular mechanism with HRP. GOx, HRP, and H_2O_2 were therefore mixed in a cuvette, the latter two in stoichiometric concentrations. After mixing, the H_2O_2 was entirely transformed into H_2O, and all the HRP, into $HRPII^+$ (see Figure 4A), and a maximum in the absorbance at 420 nm was obtained. The $HRPII^+$ variation rate is given by

$$\frac{d[HRPII^+]}{dt} = k_1^{GOx}[GOx]_t[HRP^{2+}]_t - k_3[HRPII^+]_t - k_\alpha^{GOx}[HRPII^+]_t[GOx]_t$$

During the first seconds of the decay (approximately 100 s), the $[HRP^{2+}]_t$ can be considered negligible. After integrating the

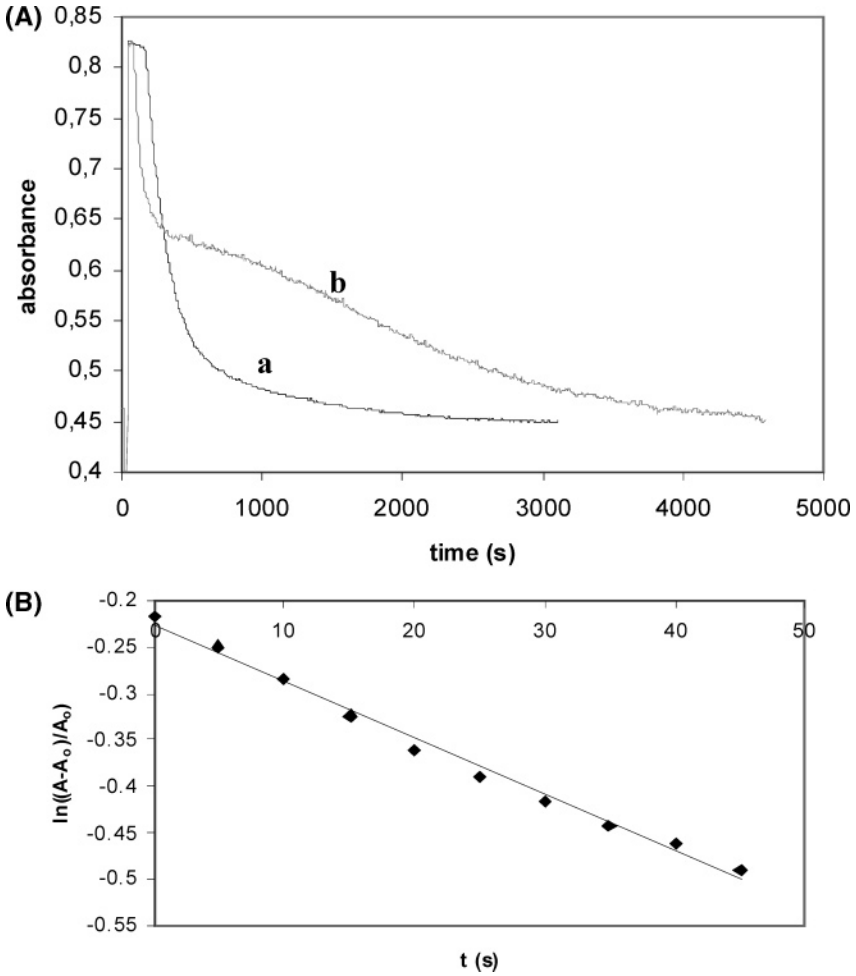

Figure 4. (A) Absorbance variation at 420 nm after mixing HRP and H_2O_2 in stoichiometric concentrations (H_2O_2 in slight excess of HRP, HRP concentration 3×10^{-5} M), (a) in the absence of and (b) in the presence of GOx (pH = 6, [GOx] = 5.0×10^{-5} M). (B) Fit of experimental results to the model proposed for the calculus of the kinetic constant k_α^{GOx}. The fit has been done by using the data corresponding to the decay curve obtained after the initial time lag (during which the slight H_2O_2 excess is consumed). The experimental data fit the following equation: $\ln(Abs_t - Abs_0/Abs_0) = -0.2267 - 0.0061t$ ($r = 0.996$).

remaining differential equation and expressing it in terms of absorbance at 420 nm, we obtained the following expression:

$$\ln \frac{Abs_t - Abs_0}{Abs_0} = \ln \frac{\Delta\epsilon}{\epsilon_{HRP}} - (k_3 + k_\alpha^{GOx}[GOx]_t)t$$

The representation of the absorbance values fits very well with this equation (Figure 4B). With the k_3 value having been previously calculated, the k_α^{GOx} obtained (after five replicate determinations) is

$$k_\alpha^{GOx} = 18 \pm 4\ M^{-1}\ s^{-1}$$

From these results we conclude that HRP reacts with GOx, the kinetic constants of the reaction being lower than those of HRP/H_2O_2. To avoid this reaction insofar as it is possible to do so, it is important that both the $[GOx]_0 < [HRP]_0$ and a long contact time between both compounds is avoided. This needs to be taken into account for various analytical methods or biochemical reactions using both enzymes or mixtures of HRP with other flavoenzymes. The results obtained for k_α^{GOx} and k_1^{GOx} demonstrated that the approximation 12 can be applied.

3.3. Glucose Reaction with Simultaneous Addition of HRP and Glucose Oxidase. (i) Molecular Absorption Signal. Figure 5 shows the absorbance variation at 420 nm over time upon addition of different glucose concentrations to a solution containing glucose oxidase GOx and HRP. [GOx]/[HRP] $\ll 1$, avoiding a reaction between them, and [glucose]/[HRP] < 1. As can be seen, when glucose is added, the absorbance increases from the initial value Abs_0 to a value Abs_{max} and then decreases gradually to return to the initial value Abs_0. From the analytical point of view the better sensitivity for glucose determination will be obtained by using ΔAbs_{420} as the analytical parameter defined as:

$$\Delta Abs_{420} = Abs_{420,max} - Abs_{420,0}$$

Similar qualitative results are obtained by working at any other wavelength in which $\epsilon_{HRPII^+} > \epsilon_{HRP}$; when the wavelength selected fulfils $\epsilon_{HRPII^+} < \epsilon_{HRP}$, the maximum turns into a minimum. This absorbance variation can be established from the reaction mechanism that takes place within HRP excess conditions. When glucose is added to the solution containing enzymes, two opposite processes take place (see Scheme 2): (a) an increase in absorbance due to $HRPII^+$ formation after hydrogen peroxide production through the glucose oxidase

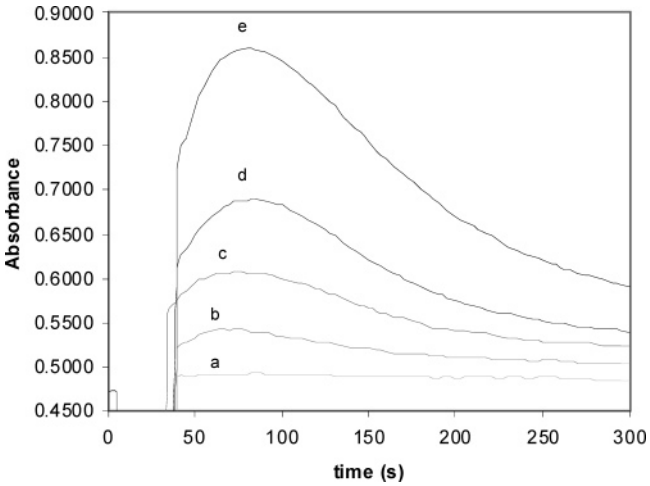

Figure 5. Changes in Abs at 420 nm as a function of G concentration (a) 7.0×10^{-6} M, (b) 1.4×10^{-5} M, (c) 2.1×10^{-5} M, (d) 2.8×10^{-5} M, (e) 4.2×10^{-5} M (pH = 6, $[HRP]_0 = 3.0 \times 10^{-5}$ M and $[GOx]_0 = 7.5 \times 10^{-7}$ M).

reaction and (b) a decrease in absorbance due to the $HRPII^+$ elimination via the intramolecular reduction process. These two opposite processes give rise to the appearance of an absorbance maximum.

(ii) Mathematical Model. Scheme 2 can be used as the starting point. Kinetically, the following assumptions can be made: (a) The GOx concentration is much lower than HRP, so the GOx/HRP reaction is negligible; (b) the initial glucose concentration is much lower than the oxygen concentration in the buffer solution so that the oxygen consumption is negligible ($[O_2]_t = [O_2]_0$); (c) as has been indicated before, the steady-state condition could be applied to $[H_2O_2]_t$ and $[GOx.H_2]_t$. The rate of the $[HRPII^+]_t$ variation with time is thus given by

$$\frac{d[HRPII^+]_t}{dt} = k_a[GOx]_t[G]_t - k_3[HRPII^+]_t - k_\alpha^{HRP}[HRPII^+]_t[HRP]_t \quad (14)$$

At the interval where maximum absorbance is reached, HRP and $HRPII^+$ coexist in significant concentrations so that simplification of eq 2 can be applied to eq 14. In addition, at the moment at which absorbance is at a maximum, $HRPII^+$ is maximal, so that eq 14 becomes

$$k_a[GOx]_t[G]_t - k_3[HRPII^+]_t - k_\alpha^{HRP}[HRPII^+]_t([HRP]_0 - [HRPII^+]_t) = 0$$

The glucose concentration at the absorbance maximum or minimum will be given by the corresponding second-order kinetic where it is taken into account that glucose oxidase is in its oxidized form throughout the interval where the absorbance changes

$$[G] = [G]_0 \exp(-k_a[GOx]_0 t_{max}) \quad (15)$$

t_{max} being the time at which absorbance is maximum or minimum. Finally, combining eqs 6, 14, and 15 yields

$$[G]_0 = \Delta Abs_{max,\lambda} \frac{(k_3 + k_\alpha^{HRP}[HRP]_0)\exp(k_a[GOx]_0 t_{max})}{\Delta\epsilon_\lambda k_a[GOx]_0} - \Delta Abs_{max,\lambda}^2 \frac{k_\alpha^{HRP}\exp(k_a[GOx]_0 t_{max})}{\Delta\epsilon_\lambda^2 k_a[GOx]_0} \quad (16)$$

This equation relates $[G]_0$ with $\Delta Abs_{max,\lambda}$ at any wavelength. As can be seen, $[O_2]_0$ does not appear in eq 16. This is a very important advantage over other enzymatic methods for glucose determination based on GOx.

(iii) Model Confirmation and Optimization of Variables for Glucose Determination. Equation 16 can be rearranged to

$$[GOx]_0 \exp(-k_a[GOx]_0 t_{max}) = \Delta Abs_{max,\lambda} \frac{(k_3 + k_\alpha^{HRP}[HRP]_0)}{\Delta\epsilon_\lambda k_a[G]_0} - \Delta Abs_{max,\lambda}^2 \frac{k_\alpha^{HRP}}{\Delta\epsilon_\lambda^2 k_a[G]_0} \quad (17)$$

To test the reliability of the model with respect to the GOx concentration, the glucose and HRP concentrations were kept constant and the GOx concentration varied. The results obtained are shown in Table 2 and were fitted according to eq 17 and the following equation obtained:

$$[GOx]_0 \exp(-k_a[GOx]_0 t_{max}) = (-1.41 \times 10^{-5})\Delta Abs_{max,\lambda}^2 + (4.44 \times 10^{-6})\Delta Abs_{max,\lambda} - (3.31 \times 10^{-9}) \; (r = 0.9990)$$

The results suggest that if the GOx concentration increases, the t_m will decrease. However, for high GOx concentrations the GOx/HRP interaction appears, rendering the absorbance versus time useless (see Figure 6) and eq 17 more complex. Several values for k_a have been reported in the bibliography, but an average of 10^4 M^{-1} s^{-1} is representative. From this equation and a study of the residuals, a k_3 value of 0.0025 ± 0.0003 M^{-1} s^{-1} and a k_α value of 289 M^{-1} $s^{-1} \pm 38$ were obtained, matching very well (t-test) with those obtained above (see section 3.1). For this work a 5.0×10^{-7} M GOx concentration was chosen for the following experiments because from this value a maximum ΔAbs is obtained, the effect of $[G]_0$ on t_m is negligible, and the GOx/HRP during the reaction time is also negligible.

In addition, calibration tests for glucose (between 5.0×10^{-6} M and 6.0×10^{-5} M) at three different wavelengths (420, 450, and 560 nm) and with three different HRP concentrations were carried out. The $[G]_o \exp(-K_a[GOx]_0 t_{max}$ versus ΔAbs_{max} representations were then compiled, and the corresponding values were fitted with the proposed model. From this the k_3 and k_α^{HRP} values can be calculated again giving

$$k_3 = 0.0041 \pm 0.0012 \; s^{-1} \qquad k_\alpha^{HRP} = 243 \pm 23 \; M^{-1} s^{-1}$$

which are statistically similar (t-text) to those previously obtained in eq 9. In our opinion, all these results validate the proposed model in eq 17.

The model predicts that the working range depends on the initial HRP concentration, given that the absorbance changes are observed for hydrogen peroxide concentrations, and therefore glucose concentrations, below the initial HRP concentration. Given that it is necessary to work with HRP concentrations at which suitable absorbance values will be obtained, the working

Table 2. Effect of GOx on ΔAbs and t_m (Experimental Conditions: λ = 420 nm, $[HRP]_0 = 2.1 \times 10^{-5}$ M, $[G]_0 = 2.8 \times 10^{-5}$ M, pH = 6)

[GOx], $\times 10^7$ M	ΔAbs	t_{max}, s
1.06	0.0622	321
3.17	0.2048	96
4.76	0.3704	79
6.88	0.4256	54
7.54	0.3648	70

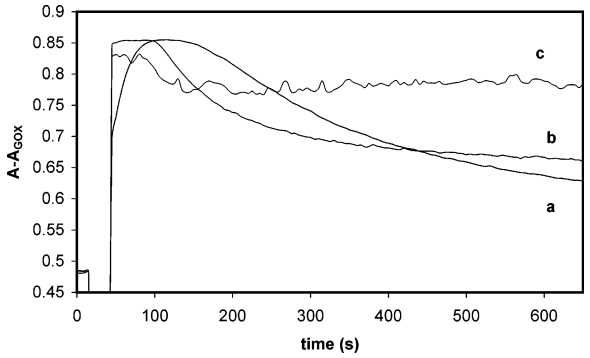

Figure 6. Absorbance variation at 420 nm working with high glucose oxidase concentrations, (a) 7.1×10^{-7} M, (b) 1.0×10^{-5} M and (c) 5.0×10^{-5} M. (pH = 6, $[HRP]_0 = 3.0 \times 10^{-5}$ M and $[G]_0 = 2.8 \times 10^{-5}$ M). The absorbance value of GOx (being constant) has been subtracted from the three signals.

range for glucose will be determined by this condition. The model proposed fits for HRP concentrations between 1.5×10^{-5} M and 6.0×10^{-5} M working with an excess of HRP with respect to glucose, as can be seen in Figure 7A. For high glucose concentrations working with a fixed HRP concentration, the absorbance change tends toward $\Delta\epsilon[HRP]_0$.

The effect of pH on the kinetic of the process was studied. In Figure 7B the values of the absorbance variation and the time needed to reach 40% HRP regeneration as a function of pH is shown. As can be seen, at pH 6 the highest percentage of absorbance variation and the shortest reaction time are obtained. It is worth noting that the overall enzymatic reaction does not consume H^+, indicating that the buffer is not strictly necessary.

(iv) Analytical Figures of Merit and Glucose Determination in Serum. For glucose determination eq 16 can be expressed as

$$[G]_0 = K_1\Delta Abs_{max,\lambda} - K_2\Delta Abs^2_{max,\lambda} \qquad (18)$$

which establishes a quadratic relation between glucose concentration and $\Delta Abs_{max,\lambda}$, for any wavelength. Figure 8 shows a graphical representation obtained in these conditions. In the conditions considered for glucose determination (see 2.3(i)), the working response range spans 2.5×10^{-6} to 5.5×10^{-5} M. The precisions of the methods (as RSD) obtained were 2.8% and 7.9% for 420 and 560 nm, respectively (1.5×10^{-5} M glucose and five replicates). By using higher HRP concentrations the upper limits of the calibration graph increase but the quantification limit is higher. Equation 18 can be linearized to $\Delta Abs_{max,\lambda} = (K_1/K_2) - (1/K_2)([G]_0/\Delta Abs_{max,\lambda})$ when the addition standard method needs to be an applied equation.

This method is particularly advantageous for samples containing proteins (i.e., biological samples) because it is less sensitive to the effect of the intermolecular regeneration of HRP

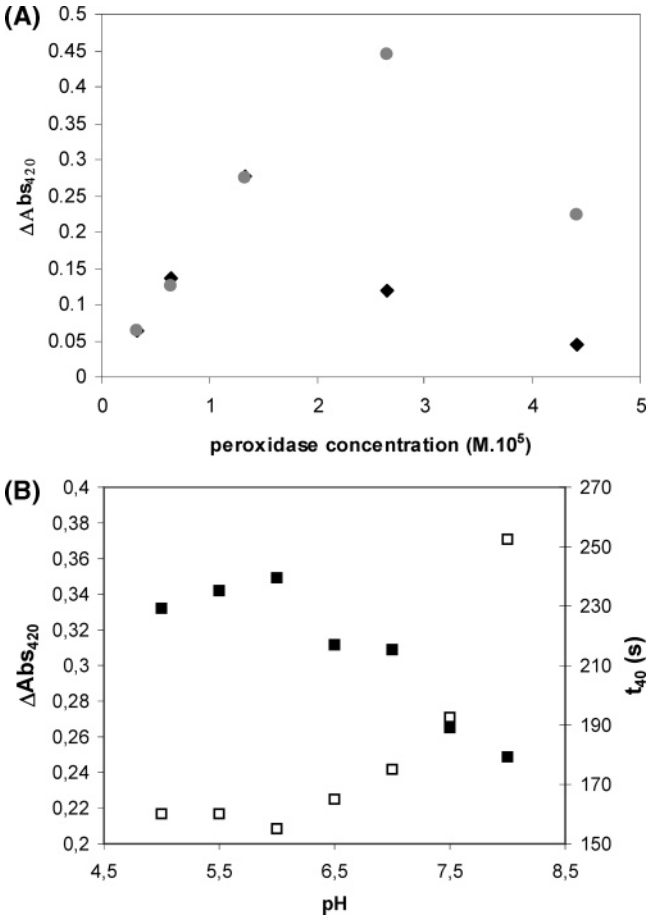

Figure 7. (A) ΔAbs_{420} variation as a function of HRP concentration for different G concentrations (pH = 6, $[GOx] = 9.7 \times 10^{-7}$ M): (◆) 1.4×10^{-5} M, (gray circles) 2.8×10^{-5} M. (B) ΔAbs_{420} variation as a function of pH ($[GOx] = 7.3 \times 10^{-7}$ M and $[G] = 2.8 \times 10^{-5}$ M): (■) ΔAbs_{420} and (□) t_{40}.

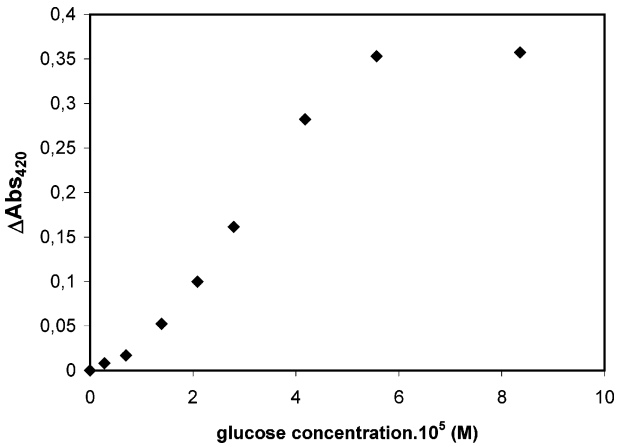

Figure 8. ΔAbs_{420} variation as a function of glucose concentration (pH = 6, $[HRP]_0 = 3.0 \times 10^{-5}$ M and $[GOx]_0 = 7.4 \times 10^{-7}$ M).

than that described below (see section 3.4). To test this, the commercial synthetic serum was used, for which the glucose concentration is not certified. For this reason a recovery study on the sample was performed. Glucose was first determined in the synthetic plasma by the present method and by a previously validated method[11] (Table 3). The results in both cases do not significantly differ (t-test, 95% confidence). Subsequently, glucose was analyzed in three samples of glucose spiked

Table 3. Glucose Concentration and Recovery Results Obtained from Different Samples (in mg L^{-1} for Synthetic Serum Sample and in g L^{-1} for Fruit Juice Samples); for Method b, See Ref 11

	glucose concentration peroxidase method	glucose concentration method b	recovery (%)
synthetic serum	585 ± 31	615 ± 25	100.4 ± 3.9
orange juice	17.2 ± 0.4	18.4 ± 0.7	102.0 ± 2.2
pineapple juice	39.3 ± 1.0	40.4 ± 0.4	95.2 ± 2.5

synthetic plasma. The quantities of glucose added and the recoveries obtained are also shown in Table 3.

3.4. Glucose Determination with HRP after Incubation with GOx. As an alternative to the procedure described above, glucose can also be determined in a two-step process. In the first step, GOx is added to a sample containing glucose and is left to react until all the glucose is oxidized and H_2O_2 is formed. In the second step, HRP is added to the sample and the absorbance variation is monitored. Tests have been carried out with different GOx concentrations, and 5×10^{-7} M was finally selected to avoid the HRP/GOx reaction (the HRP concentration was 2×10^{-5}M); for this concentration 5 min was sufficient for the quantitative conversion of glucose to H_2O_2. After incubation, the HRP addition gave Abs versus time representations similar to those shown in Figure 2A. By working at pH = 6, a linear response range between $\Delta Abs_{0,\lambda}$ and a glucose concentration in the range 2.8×10^{-6} to 5.6×10^{-5} M was obtained, in accordance with the following equation:

$$\Delta Abs_{0,\lambda} = 31\,023[Glucose]_0 \qquad r = 0.9991$$

As can be seen, the slope of this calibration line matches very well with equation 8 and the values indicated in Table 1. This indicates that the peroxidase/H_2O_2 mathematical model previously described can be applied in the incubation method when low GOx concentrations are used.

This method can be applied for glucose determination where there is a low concentration (or an absence) of proteins. As an example, glucose in three commercial fruit juices was determined in this way and also by a previously validated method[11] (Table 3). The results in both cases do not significantly differ (t-test, 95% confidence). The same samples were then spiked with glucose and analyzed again. The amount of glucose added and the recoveries obtained are also shown in Table 3.

4. Summary

The kinetic mechanism of HRP with H_2O_2 has been studied, and the kinetic constants were obtained. It is demonstrated that HRP can be used as an analytical reagent for a simple method of H_2O_2 determination. The interaction of HRP with GOx has also been demonstrated, a kinetic model was developed, and the constants were obtained. The same methodology can be applied to study interactions between other flavoenzymes and heme-proteins (i.e., hemoglobin). From the analytical point of view, this result is very important because it draws attention to the problems than can be appear when HRP and GOx (or other flavoenzymes) are previously mixed in enzymatic determinations. Finally, the paper demonstrates that HRP can simultaneously be used as a colorimetric reagent in enzymatic methods involving H_2O_2 previously formed from the analyte, the glucose reaction with GOx being used as a model. As the reaction can be followed after adding GOx and HRP to the glucose sample, this methodology can easily be implemented in sensors, for example via polyacrylamide[25] or sol−gel encapsulation,[26] in which the HRP properties will be used for detecting the reaction. Regeneration of the sensor could be accomplished by an external reducing agent to increase its lifetime. New directions in this line of research include studying the possibility of substituting HRP by hemoglobin (i.e., blood samples) and using these properties for analytical determinations of glucose or other analytes.

Acknowledgment. This work was supported by the DGES (Ministerio de Ciencia y Tecnología of Spain); Project BQU 2003-04646). V.S. thanks the DGES for a grant.

JA046830K

(25) Sanz, V.; Galbán, J.; de Marcos, S.; Castillo, J. R. *Talanta* **2003**, *60*, 415−423.
(26) Smith, K.; Silvernail, N. J.; Rodgers, K. R.; Elgren, T. E.; Castro, M.; Parker, R. M. *J. Am. Chem. Soc.* **2002**, *124*, 4247−4252.